The Mean Received Power in *Ad Hoc* Networks and Its Dependence on Geometrical Quantities

Jan Hansen, *Student Member, IEEE,* and Peter E. Leuthold, *Member, IEEE*

***Abstract*—System-level simulations for *ad hoc* networks require the mean power that is received by an arbitrary unit of the piconet as an input parameter. Since the radio channel in piconets depends strongly on the environment in which two communicating units are located, easily applicable models for the mean received power must be determined by a few relevant, explicitly geometrical quantities. Starting from a very general description of the stochastic radio channel by an integral equation, it is shown that these quantities are the surface area and the volume of the domain in which the transmitter and the receiver can move. On the basis of an exponential pathloss model with pathloss exponent q, a lower and an upper bound for the mean received power are derived. The resulting analytical expressions are highly flexible and allow a quick calculation of bounds for the mean received power in many practically relevant cases.**

***Index Terms*—Ad hoc networks, mean received power, stochastic channel modeling, wave propagation.**

I. Introduction

DURING recent years, there has been a growing interest in *ad hoc* networks such as IEEE 802.15 (Bluetooth) or IEEE 802.11. In contrast to networks with fixed access points, the former are self-organizing within a piconet. Knowledge about the radio channel is required for the design and test of such a system. Of particular importance is the mean received power (MRP); since results from numerous measurement campaigns indicate that the received power is lognormal distributed [1], the MRP is a fundamental quantity for stochastic channel models as well as for system-level simulations. It refers not only to the power between two communicating units. Any link between two communicating units is a source of interference for other units, and the ongoing discussion about the coexistence of Bluetooth and IEEE 802.11b [2] requires in particular information about the mean interference power. Since there is no clear hierarchy between the users of a piconet, both quantities can from the viewpoint of wave propagation be treated in a similar manner.

Clearly, the MRP depends strongly on the environment in which the system operates. A flexible model with general applicability must thus allow a choice between different types of architecture; it has, in addition to the wave propagation aspects, to use explicitly geometrical parameters. All common stochastic models, however, depend on geometrical parameters only on a very intuitive level. They often rely on data derived from measurements in some different scenarios. The received power is, for instance, treated in terms of pathloss models [3]–[5], i.e., an average over a number of environments is obtained, but the distance between T_x and R_x is fixed. In other models a somewhat artificial definition of propagation scenarios in terms like "small rooms," "large rooms," etc. [6], [7] is applied. The opposite holds for ray tracing models, which are based on completely defined environments. This approach hence does not directly lead to a stochastic model; strictly speaking, those that are derived from ray tracing [8] are only valid for the single environment for which the ray tracer was run. But for such an integral quantity as the MRP, this approach seems to need a large computational effort; therefore the question arises as to whether it is possible to achieve reasonable results with a simpler calculation scheme.

A step in this direction has been made in [9], where methods from geometric probability [10]–[12] were applied in order to significantly simplify a ray tracing algorithm that was used for the prediction of the received power within a building. As the model operates site-specifically, it requires several site-related input parameters and can only numerically be evaluated. Furthermore, it is restricted to buildings composed of rectangular substructures.

This paper shows that the MRP as required for statistical channel models can be analytically derived. The obtained formulas rely strongly on methods from geometric probability and allow the calculation of the MRP not only for rectangular but also for arbitrary convex domains, of which only the volume and the surface area must be known. The starting point is a very general description of the stochastic radio channel as a deterministic function for wave propagation, which operates on stochastically defined variables such as random positions of transmitter (T_x) and receiver (R_x), combined with the geometry of the environment. If the deterministic part is described by a simple pathloss model, integral expressions arise that appear in channel modeling not only for the presently discussed case but also for other pathloss models, other network types, and other quantities than just the MRP. Their solution is carried out in the second section of this paper. In the third part, the resulting bounds are tested by simulations. An Appendix gives additional details.

II. Theory

One aim of stochastic channel modeling is to find conditional distributions $P(\xi|\Gamma)$ of particular channel parameters ξ or any of their kth moment, $E[\xi^k|\Gamma]$. The parameter Γ denotes any environment for which the model is developed. An environment is usually characterized like "a floor of a building" or "office environment," and can hence be described by a set of precisely

Manuscript received December 21, 2001; revised June 7, 2002.

The authors are with the Communication Technology Laboratory, Swiss Federal Institute of Technology (ETH), Zurich, Switzerland (e-mail: hansen@nari.ee.ethz.ch; leuthold@nari.ee.ethz.ch).

Digital Object Identifier 10.1109/TAP.2003.816376

defined environments $\gamma \in \Gamma$, where "precisely" means sufficiently accurate for a correct simulation of the electric field distribution. The quantity ξ can be, for instance, an amplitude, an angle of arrival, or even an entire set of useful parameters. It is random, since the positions of R_x and T_x are random in γ. Since wave propagation is a function of the positions of R_x, T_x, and γ, one can express the stochastic nature of the radio channel using the law of total probability [13]

$$\begin{aligned} P(\xi|\Gamma) &= \frac{1}{V_{T_x} V_{R_x} |\Gamma|} \sum_{\gamma \in \Gamma} \int_{D_{T_x}} \mathrm{d}p_{T_x} \int_{D_{R_x}} \mathrm{d}p_{R_x} \\ &\quad \times P(\xi|p_{T_x}, p_{R_x}, \gamma) p(p_{T_x}, p_{R_x}) \\ E[\xi^k|\Gamma] &= \frac{1}{V_{T_x} V_{R_x} |\Gamma|} \sum_{\gamma \in \Gamma} \int_{D_{T_x}} \mathrm{d}p_{T_x} \int_{D_{R_x}} \mathrm{d}p_{R_x} \int_{\Xi} \mathrm{d}\xi \\ &\quad \times \xi^k p(\xi|(p_{T_x}, p_{R_x}, \gamma) p(p_{T_x}, p_{R_x}). \end{aligned} \tag{1}$$

In these two equations, D_{T_x} is a domain of volume V_{T_x} in which T_x is distributed; D_{R_x} is a domain of volume V_{R_x} in which R_x is distributed; and the density $(1/(V_{T_x} V_{R_x}))p(p_{T_x}, p_{R_x})\mathrm{d}p_{R_x}\mathrm{d}p_{T_x}$ describes the probability that T_x and R_x are located at some points p_{T_x} and p_{R_x}. The expression $|\Gamma|$ denotes the number of elements in Γ and normalizes the sum over all environments. The domain Ξ is that in which the moments of ξ are calculated.

All deterministic models require the environment γ to be completely defined; in this case, the expression $P(\xi|p_{T_x}, p_{R_x}, \gamma)$ is a unit step function in several dimensions and the evaluation of (1) becomes equivalent to Monte-Carlo ray tracing [8], [14]. Empirical models, on the other hand, are valid for an entire set of γ, which is equivalent to the summation over all $\gamma \in \Gamma$ of the term $P(\xi|p_{T_x}, p_{R_x}, \gamma)$ within the integral. This is done in the case of the well-known empirical pathloss model [15]–[17], which states that the pathloss obeys a power law of the form

$$\langle \mathcal{P}_{R_x} | r, q, \kappa \rangle = \kappa \frac{1}{r^q} \tag{2}$$

where $\mathcal{P}_{R_x}$ is the received power, κ is a constant, r is the distance between T_x and R_x, and q is the pathloss exponent. The brackets $\langle .|. \rangle$ clarify that this model is an empirical model, which is valid in all sets of environments Γ that can be parameterized by particular q and κ.

The integral expression (1) gives a starting point from which various channel models can be deduced by applying various assumptions about the environment, its wave propagation characteristics, and the distribution of T_x and R_x. The possible positions define the boundaries of the integral in (1); the expression is hence of geometrical nature, and geometrical methods are needed to solve it for specific cases.

In this paper, (1) is solved for a low-power *ad hoc* network. For the description of wave propagation, the pathloss model (2) is a suitable and simple starting point; the environment is not explicitly characterized but in fact parameterized by the pathloss exponent q and by κ. For most situations in low-power networks, q is in the range around two and thus not much higher than the pathloss in free space.

In an *ad hoc* network, all users are uniformly distributed within the same particular domain D, e.g., a part of a building. For the following derivation, no assumption is required about the particular shape of D; it must, however, be convex, i.e., for each pair of points in D, the line segment that connects these points belongs also to D. This assumption is not a severe drawback for the applicability of the model.

The MRP, i.e., the expectation of the received power for any two communicating units 1 and 2 then equals the integral

$$I_q = E\left[\frac{\kappa}{r^q}\right] = \frac{\kappa}{V\tilde{V}} \int_D \int_{D \backslash B_\rho(p_2)} \frac{1}{r^q} \mathrm{d}p_1 \mathrm{d}p_2. \tag{3}$$

In this expression, the differential $\mathrm{d}p_i$ denotes the density of the position of user i. The integration domain for p_1 is not D but $D \backslash B_\rho(p_2)$, i.e.,a ball of radius ρ is cut out around p_2. This ball ensures that the distance r between p_1 and p_2 cannot be smaller than ρ, which is important for the application of the pathloss model (2). This model is valid only in the far-field of the antenna, where the field decays in free space with $1/r$. The factor $V\tilde{V}$ normalizes the density $\mathrm{d}p_1\mathrm{d}p_2$ to one; the entire volume of D is denoted by V, and the volume of $D \backslash B_\rho(p_2)$ by $\tilde{V}$.

Integral (3) is of a fundamental type, since it describes a $1/r^q$ interaction between two point-like particles. It hence occurs in numerous fields like statistical physics and solid-state physics [18], [19]. Attempts to solve or to bound this integral in two dimensions and for general or particular shapes of D reach back many decades [20], [21]. Explicit solutions in three dimensions, however, are very hard to achieve and depend strongly on the shape of D [22]. Explicit solutions, however, do not seem necessary, since one may already intuitively claim that due to the double integration in (3) more robust approximations should exist. The discovery that specific integrals of the above type are indeed independent from the particular shape, but are only determined by quantities like the surface or the perimeter of D, was first made in two dimensions [23]. This and some related results stimulated the development of a new mathematical branch called integral geometry; after some decades numerous techniques for the solution of problems that arise at the boundary between probability theory and geometry were developed [10]–[12], [24], [25] and are still under investigation today.

The key strategy for tackling (3) is the transformation of the densities of points $\mathrm{d}p_1$ and $\mathrm{d}p_2$ into the densities of two points on a line G and the density of this line, $\mathrm{d}G$. The derivation of $\mathrm{d}G$, its rigid treatment, and the proof that $\mathrm{d}G$ is a well and uniquely defined measure requires techniques from differential geometry and group theory [10]. Its geometrical meaning can, however, be quickly outlined (Fig. 1). The perpendicular of the line G to the origin O defines a distance $\tilde{r} = \|p_0\|$ of G to O. The line segment $\overline{Op_0}$ lies in the plane F, which is also perpendicular to G and thus uniquely defined. The point of intersection p_0 of G with F can be described on F in cylindrical coordinates by its distance $\tilde{r}$ from O and an angle ϕ relative to a fixed axis of F, here x. Furthermore, G has a direction that can be described by the pair of angles (ψ, θ). The density of lines is the volume element of F at p_0, combined with the volume element of the unit sphere $\mathrm{d}G = \tilde{r}\mathrm{d}\tilde{r}\mathrm{d}\phi \cdot \sin\theta \mathrm{d}\theta\mathrm{d}\psi$. This density is motion invariant, i.e., it does not depend on the location of O.

Using $\mathrm{d}G$, the density of the location of two points p_1 and p_2, given in Cartesian coordinates, can be transformed into the density of these points on G, multiplied with $\mathrm{d}G$; equivalent to

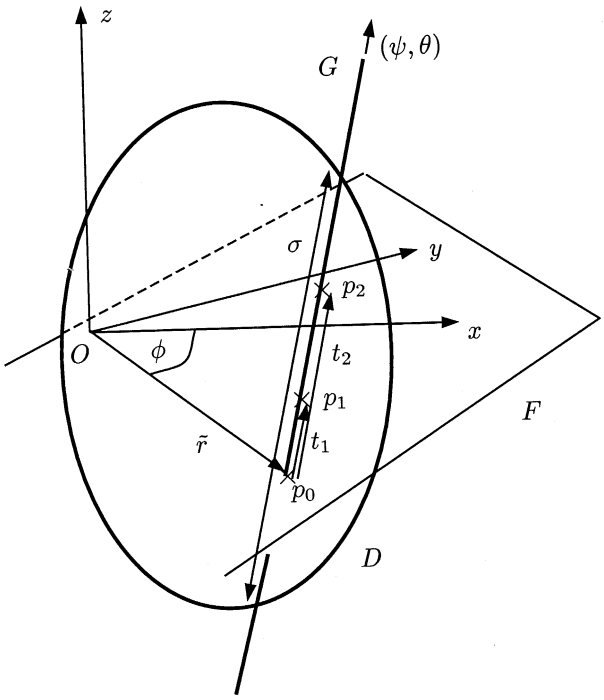

Fig. 1. Sketch of the two points p_1 and p_2 on the line G.

the transformation of the location of a single point from Cartesian to spherical coordinates, the expression must be weighted with the square of the distance between p_1 and p_2, so that one obtains $\mathrm{d}p_1\mathrm{d}p_2 = |t_2 - t_1|^2 \mathrm{d}t_1\mathrm{d}t_2\mathrm{d}G$, where t_1 and t_2 are the coordinates of the points relative to p_0 on G. Hence, (3) can be written as

$$I_q = \frac{\kappa}{V\tilde{V}} \int_D \int_{D\setminus B_\rho(p_2)} \frac{1}{r^q} \mathrm{d}p_1 \mathrm{d}p_2 = \frac{\kappa}{V\tilde{V}} \int_{D\cap G\neq\emptyset} \int_{t_1\in D\cap G\setminus B_\rho(p_2)} \int_{t_2\in D\cap G} r^{2-q} \mathrm{d}t_1\mathrm{d}t_2\mathrm{d}G \quad (4)$$

where $r = |t_2 - t_1|$ and the line segment $\{t_i | t_i \in D\cap G\}$ arises from the intersection of D with G and defines the integration domain for t_1 and t_2. Note that for t_1 this line is split in two rays, since p_1 cannot be inside the ball $B_\rho(p_2)$.

The integral over $\mathrm{d}G$ is now an integral over the lines that intersect D. Integration of (4) over all $t_1, t_2 \in D, t_1 \notin B_\rho(p_2)$, yields for a convex domain

$$I_q = \frac{2\kappa}{(3-q)(4-q)V\tilde{V}} \times \left\{ \int_{\sigma>\rho} \sigma^{4-q}\mathrm{d}G + (3-q)\rho^{4-q} \times \int_{\sigma>\rho} \mathrm{d}G - (4-q)\rho^{3-q} \int_{\sigma>\rho} \sigma \mathrm{d}G \right\}. \quad (5)$$

In this expression, σ is the length of the chord $\{D\cap G\}$ that arises when line G intersects D (Fig. 1). The integral does not actually extend over all lines G that intersect D, $\{(G\cap D)\neq\emptyset\}$, but only over all lines that intersect D with a chord at least of length $\sigma \geq \rho$ ($\{(G\cap D)\neq\emptyset, \sigma\geq\rho\}$). This condition arises again due to the minimum distance ρ, which must be kept between both units of the network.

Equation (5) consists of three terms. For $\rho = 0$ only the first remains. However, this term diverges for $q \longrightarrow 3$, since the integral expression of this term has a finite value, and the denominator tends to zero. The remaining two terms are thus required to keep the entire expression bounded.

Expression (5) can now be tackled with the aid of the following relations, which are valid for integrals over the density of lines [10]:

$$\int_{D\cap G\neq\emptyset} \mathrm{d}G = \frac{O_{n-2}}{(n-1)O_0} A \quad (6)$$

$$\int_{D\cap G\neq\emptyset} \sigma \mathrm{d}G = \frac{O_{n-1}}{O_0} V \quad (7)$$

$$\int_{D\cap G\neq\emptyset} \sigma^{n+1} \mathrm{d}G = \frac{n(n+1)}{2} V^2 \quad (8)$$

where O_n is the surface of the n–dimensional unit sphere and A the surface area of the convex body D with volume V. It holds that $O_n = (2\pi^{(n+1)/2})/(\Gamma((n+1)/2))$ [10], so that one has $O_2 = 4\pi$, which is the surface of the unit sphere, $O_1 = 2\pi$, which is the perimeter of a circle, and $O_0 = 2$. This triple of equations reveals that certain integrals over the density of lines over a convex body do not depend on the particular shape of the body, but only on the very integral quantities volume and surface area.

Equations (6)–(8) can be applied to solve (5). The required exponent $(4-q)$ of the chordlength σ of the first term in (5) is obtained by applying Hölder's inequality [26], which is demonstrated in the Appendix. Strictly speaking, the three relations can only be applied for $\rho = 0$, since the integration domain in (6)–(8) includes all lines, and not only those that fulfill $\sigma > \rho$. For their application in the case of $\rho > 0$, the volume and surface of that convex body is required that emerges from D when all parts of D that can be covered by the lines for which $\sigma < \rho$ are removed. This body is hard to determine if the shape of D is unknown. For particular domains, such as rectangles, the difference between the two bodies can be shown to be not large (as the MRP is given in dB scale) as long as the diameter 2ρ of the sphere $B_\rho(p_2)$ is smaller than the smallest diameter of D and the largest diameter is at least twice as large as 2ρ. In the following, this difference is neglected, and (6)–(8) are directly applied to solve (5). The validity of this approach is verified through simulations.

Using (6)–(8) and the result obtained in the Appendix, one obtains as approximate bounds for the MRP

$$\frac{2\kappa}{(3-q)(4-q)} \left\{ 2^{7-2q}\pi V^{2-q} A^{q-3} + (3-q)\rho^{4-q} \frac{\pi}{2}\frac{A}{V^2} - (4-q)\rho^{3-q}\frac{2\pi}{V} \right\} \lesssim I_q \lesssim \frac{2\kappa}{(3-q)(4-q)} \left\{ 6^{1-\frac{q}{4}} \left(\frac{\pi}{2}\right)^{\frac{q}{4}} V^{-\frac{q}{2}} A^{\frac{q}{4}} + (3-q)\rho^{4-q} \times \frac{\pi}{2}\frac{A}{V^2} - (4-q)\rho^{3-q}\frac{2\pi}{V} \right\} (q<3) \quad (9)$$

where the $\lesssim$ sign is required, since $\tilde{V}$ has been replaced by V. For $\rho = 0$, $\lesssim$ can be replaced by $\leq$.

The results seem complicated because of the possible irrationality of the exponent q. For some numbers, the expression simplifies significantly, e.g., for $q = 1$ (the mean received field strength in line-of-sight) and $q = 2$, one obtains

$$\kappa\frac{32\pi V}{3A^2} + \frac{\kappa\pi\rho^2}{V}\left\{\frac{A\rho}{3V} - 2\right\}$$
$$\lesssim E\left[\frac{\kappa}{r}\right] \lesssim \kappa\sqrt[4]{\frac{4\pi A}{3V^2}} + \frac{\kappa\pi\rho^2}{V}\left\{\frac{A\rho}{3V} - 2\right\}$$
$$\kappa\frac{8\pi}{A} + \frac{\kappa\pi\rho}{V}\left\{\frac{A\rho}{2V} - 4\right\}$$
$$\lesssim E\left[\frac{\kappa}{r^2}\right] \lesssim \kappa\frac{\sqrt{3\pi A}}{V} + \frac{\kappa\pi\rho}{V}\left\{\frac{A\rho}{2V} - 4\right\}. \qquad (10)$$

In these cases, the bounds depend in a very simple way on the volume and the surface area of D. On the one hand, such a simple dependency seems surprising. On the other, these bounds are merely a rigid formulation of the robustness of the radio channel against changes in the environment. Any measurement campaign is in fact based on the assumption that its results, which arise from a particular way of moving T_x and/or R_x in a chosen environment, are valid representatives for any environment that is geometrically similar; if this assumption did not hold, results from campaigns in similar environments would not be comparable. The fact that they are comparable is simply expressed by (9) and (10).

III. Simulations

A. Examination of the Bounds

For the examination of the bounds, a simple simulation tool was developed. This tool uniformly distributes two points, the R_x and the T_x of the *ad hoc* network, in a rectangular domain D with sidelengths a, b, and c, constrained to a given minimum distance ρ between the points. In combination with any pathloss exponent q, the mean $E[\kappa/r^q]$ can easily be evaluated from the samples of the distance r between the points. In the following, this tool is used to examine the properties of the analytical bounds with regard to ρ, to the dimensions of D, and to the value of the pathloss exponent q. All simulation results are based on 10 000 realizations of R_x and T_x positions; the constant κ equals one.

In Figs. 2 and 3, the dependence of the bounds on the dimensions of D and on the minimum distance ρ are investigated. The setup resembles an *ad hoc* network that includes all devices between 1.0 and 2.0 m height. In Fig. 2, D has a length of 4 m and a height of 1 m, and ρ equals zero; in Fig. 3, the dimensions of D are the same, but $\rho = 0.5$ m. In both figures, the width of the rooms is increased from 4 to 28 m. The analytically calculated bounds are displayed by dashed lines and circles, whereas the simulated mean is shown by a continuous line and triangles. The pathloss exponent is $q = 2$.

The bounds are comparably tight. The simulated values differ by about 1–6 dB from the lower and the upper bound; they tend to be closer to the lower bound, which is for $\rho = 0$ always within 1–3 dB distance. The bounds are better if the domain is more cubic, i.e., the ratio of the sidelengths is closer to one. For a very flat disc, the upper bound actually becomes arbitrarily bad, since A remains about constant and $V \longrightarrow 0$; according to (9), the bound tends then to infinity. The decrease in the simulated mean due to the difference in ρ is about 2 dB, which means that for $q = 2$ and the given size of D it is not strongly effected by ρ. The upper bound in Fig. 3 is also up to 2 dB lower than in Fig. 2, whereas the lower bound has lost at least 4 dB. The reason is the correcting terms for $\rho > 0$ in (9), which are equal for both bounds on linear scale and thus weigh stronger in dB for smaller values.

The dependence of the bounds and the simulated values on ρ and on q is examined for a domain of size $10 \times 5 \times 1$ m and $\rho = 0.5$ m. Notice that for $q > 2$ the domain needs not necessarily refer to a single room with free space pathloss; it can be any environment that does not encompass the given size of D and whose interior structure is absorbed into the value of q. The volume and the surface area refer again to the domain in which T_x and R_x are uniformly distributed, and are thus only indirectly related to the volume and the surface area of the actual rooms of the indoor environment.

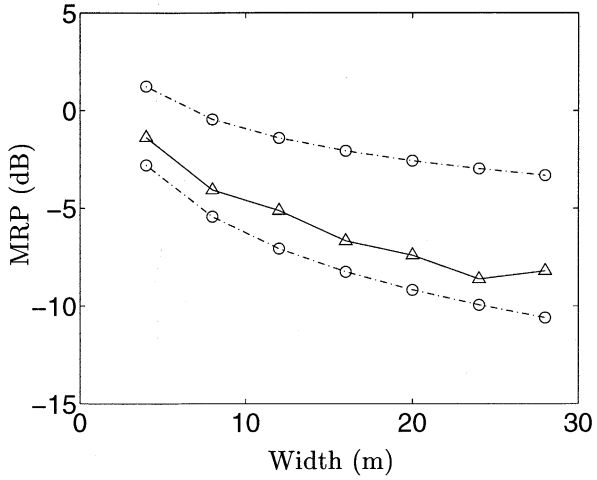

Fig. 2. MRP and analytical bounds for $\rho = 0$ m, $q = 2$, and a domain of 4 m length, 1 m height, and variable width.

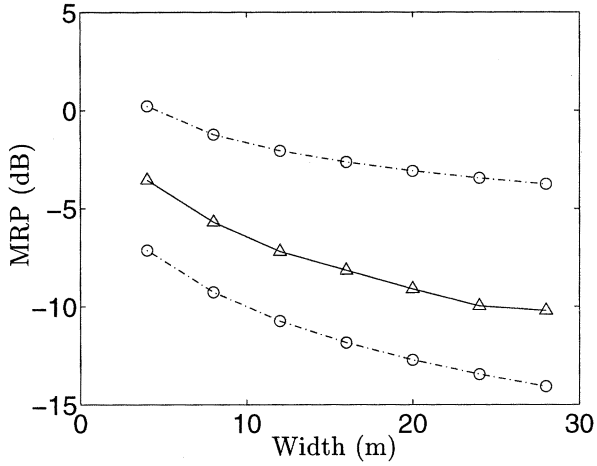

Fig. 3. Analytical bounds for $\rho = 0.5$ m, $q = 2$, and a domain of 4 m length, 1 m height, and variable width.

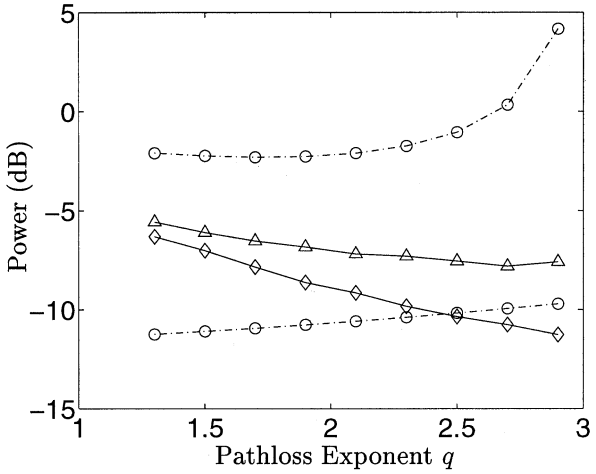

Fig. 4. Analytical bounds (circles) for values of q between 1.3 and 2.9, and $\rho = 0.5$ m. The MRP is shown for $\rho = 0.5$ m (triangles) and $\rho = 1$ m (diamonds).

The results are shown in Fig. 4. The simulated mean for $\rho = 0.5$ m (triangles) decreases slowly with increasing q. The upper bound is tightest for low q, with about 3 dB difference; the difference increases for increasing q. The lower bound is farthest apart from the simulated mean for low q and approaches it as q increases. Without the correcting terms in (9) for $\rho > 0$, both bounds would diverge. If these terms are included, the lower bound is kept below the simulated mean; the upper bound, however, still diverges. For $q > 2.5$, the upper bound is very loose. For the geometrical reasons outlined in Section II, ρ cannot be chosen larger than 0.5 m for the given domain of height 1 m. The impact of this disadvantage of the model is, within limits, not tremendous. The diamond marked line in Fig. 4 is the simulated mean for $\rho = 1$ m. This mean decreases faster than the simulated mean for $\rho = 0.5$ m and crosses the lower bound for this ρ at $q = 2.5$. The deviation between the two means increases with increasing q; it is hardly noticeable for $q = 1.5$, but reaches 4 dB for $q = 2.9$. At $q = 2$, it is about 2 dB and still well above the lower bound. The expressions for a particular ρ are hence also valid for a larger ρ, where the lower bound serves rather as a good practical approximation.

B. Comparison With Ray Tracing

The derived bounds are compared with ray tracing results. The used ray tracer relies on a Monte Carlo technique and is designed for the calculation of quantities of the stochastic radio channel [14]. For the investigation of the bounds, simulations are carried out at 2.4 GHz; empty rooms with various floor sizes of 30×8, 30×4, 20×8, 20×4, 12×8, 8×8, and 4×4 m^2 are used. All rooms are 4 m high. The positions of T_x and R_x are randomly created according to a uniform distribution, the bounds of which are the walls of the room, and a height 0.8 and 2.0 m above the floor of the rooms. The building materials are also randomly chosen; the distribution corresponds to a rather heavily constructed, old-fashioned office room with 70% concrete, 20% glass, and 10% light concrete building material. The dielectric constants are $\underline{\epsilon} = 5.5 - j0.10$ for heavy concrete [27], $\underline{\epsilon} = 5.0 - j0.025$ for glass [28], and $\underline{\epsilon} = 2.2 - j0.15$ for light concrete [27]. The dielectric constants of the first and the last material are valid at 2.4 GHz, and that of glass at 3 GHz. The antennas are isotropic, which corresponds, in the case of linear polarization, to a uniformly distributed orientation of the antennas and is a realistic assumption for an *ad hoc* network. Field vectors are transmitted and received either both parallel to the floor of the rooms, or both parallel to the walls of the room. In each run of the ray tracer, 2048 realizations of R_x and T_x positions are simulated. The MRP for each realization is calculated, using the power of the direct path and all reflections up to the second order. Again $\rho = 0.5$ m $\simeq 4\lambda$ at this given wavelength λ is set, which is almost the maximum ρ allowed for a domain of width 1.2 m. For the ray tracing simulations the distance is slightly more relaxed to 8λ, so that the far-field condition is fulfilled for all antennas with aperture smaller than 2λ [29] (see also Fig. 4). The pathloss model (2) is fitted to the result. The obtained pathloss exponents are all between about 1.7 and 1.9, and the value of κ about -41 dB. This is realistic, since in environments with a strong direct path and many reflections, the pathloss exponent q is known to be a bit lower than two, and the received power in 1 m distance from an isotropic antenna is $\lambda^2/(4\pi)^2 = -40$ dB for 2.4 GHz. The analytic bounds are then calculated using the obtained values for q and κ; the volume V and the surface area A result from the floor size and the height of the domain in which R_x and T_x can move. As their locations are restricted between 0.8 and 2.0 m above the floor, this height equals 1.2 m

TABLE I
MRP $\mathcal{P}_{R_x}$ FOR THE TRANSMITTED AND RECEIVED COMPONENT BEING PARALLEL TO THE WALLS AND CORRESPONDING BOUNDS FOR ROOMS OF 4M HEIGHT AND DIFFERENT FLOOR SIZE

floor size (m^2)	30×8	30×4	20×8	20×4	12×8	8×8	4×4
upper bound (dB)	-47.4	-46.0	-46.3	-44.5	-44.6	-43.8	-40.7
$\mathcal{P}_{R_x}$ (‖ to walls) (dB)	-50.0	-51.1	-51.1	-49.4	-49.5	-48.5	-44.2
lower bound (dB)	-57.5	-55.8	-55.6	-53.3	-52.8	-51.4	-47.0

TABLE II
MRP $\mathcal{P}_{R_x}$ FOR THE TRANSMITTED AND RECEIVED COMPONENT BEING PARALLEL TO THE FLOOR AND CORRESPONDING BOUNDS FOR ROOMS OF 4M HEIGHT AND DIFFERENT FLOOR SIZE

floor size (m^2)	30×8	30×4	20×8	20×4	12×8	8×8	4×4
upper bound (dB)	-47.4	-45.4	-46.3	-44.4	-45.0	-43.9	-40.8
$\mathcal{P}_{R_x}$ (‖ to floor) (dB)	-50.2	-50.9	-50.7	-49.5	-49.3	-48.2	-44.5
lower bound (dB)	-57.7	-55.2	-55.6	-53.2	-53.4	-51.6	-47.1

In Tables I and II, the ray tracing results are compared to the analytic bounds, where each table displays the values obtained from a particular state of polarization. The results for the two states of polarization are very similar. The validity of the model is clearly demonstrated. For the seven investigated scenarios, the simulated powers are between the analytically calculated bounds.

The simulation results also indicate that the fit parameter κ can be replaced by the pathloss in 1 m distance, $\lambda^2/(4\pi)^2$. This substitution makes the model much easier to apply; it then depends only on q, which can be chosen to represent a particular scenario, the wavelength, and the dimensions of D.

IV. Conclusion

Analytical bounds on the mean received power in *ad hoc* networks are presented. The bounds are sufficiently tight for many relevant cases. Scenarios are characterized only by their pathloss exponent q, the pathloss in 1 m distance or the wavelength, respectively, and the surface area and the volume of the domain, in which the units of the communication system can move. Thus the bounds can be applied very conveniently, since a system designer needs only minimum information about the environment in which the *ad hoc* networks operates. No classification of a radio environment is required. The bounds do not require any empirical input, and their validity for a typical *ad hoc* network scenario is demonstrated with ray tracing data.

A drawback is that the upper bound diverges for $q \longrightarrow 3$, even though correcting factors are introduced to keep T_x and R_x a minimum distance ρ apart. But whereas the upper bound becomes unreliable in this region, the lower bound actually approaches the MRP and is a good approximation. Also, the presented bounds are valid only for $q < 3$, but for many environments higher pathloss exponents are common. However, an extension of the bounds to arbitrary q is already under investigation.

The model presented is a specific case derived from a very general integral expression that characterizes the stochastic radio channel. The integral contains all necessary field theoretical and geometrical information that is required to derive stochastic channel properties. The crucial part is the derivation of a solution for specific cases. The solution need not necessarily be analytical, but can also be obtained numerically. Once it is obtained, the resulting expressions have the advantage that they are very general and free of any intuitive character, since they do not rely on data or simulation results that refer to particularly chosen scenarios.

In this case, the geometrical part of the integral can be solved by integral geometric methods that have not previously been applied to channel modeling. The potential benefit of integral geometry for stochastic channel modeling seems to be high, since the solution strategies that have been developed in this field are anything but exhausted so far. As similar types of integrals arise for the radio channels of communication systems with a fixed access point or for more ray-tracing-like wave propagation models, the application of an integral description of the radio channel and its solution with geometrical methods seems promising for the future development of stochastic channel models.

Appendix

Hölders inequality [26] applied to an integral over two functions $f \geq 0$ and $g \geq 0$ and the density of lines $\mathrm{d}G$ is

$$\int\limits_{D\cap G\neq\emptyset} f\cdot g\mathrm{d}G \leq \sqrt[l]{\int\limits_{D\cap G\neq\emptyset} f^l \mathrm{d}G}\ \sqrt[l']{\int\limits_{D\cap G\neq\emptyset} g^{l'}\mathrm{d}G} \quad (11)$$

where $(1/l)+(1/l')=1$ and $l\geq 1$. Using (11), a lower and an upper bound for the integral

$$\int\limits_{D\cap G\neq\emptyset} \sigma^{4-q}\mathrm{d}G \quad (12)$$

can be derived as follows.

For the lower bound, set $f=\sigma$, $g=1$ on the left-hand side of (11), and choose $l=4-q$. Then $l'=(4-q)/(3-q)$, and

$$\int\limits_{D\cap G\neq\emptyset} \sigma\mathrm{d}G \leq \left(\int\limits_{D\cap G\neq\emptyset} \sigma^{4-q}\mathrm{d}G\right)^{\frac{1}{4-q}} \left(\int\limits_{D\cap G\neq\emptyset} 1\mathrm{d}G\right)^{\frac{3-q}{4-q}} \quad (13)$$

and the lower bound for $\int \sigma^{4-q}\mathrm{d}G$ can easily be evaluated using (6) and (7).

For the upper bound, set $f=\sigma^{4-q}$, $g=1$, on the left-hand side of (11), and choose l such that $(4-q)l=(3+1)$; one obtains $l=(1-(q/4))^{-1}$, $l'=4/q$, and

$$\int\limits_{D\cap G\neq\emptyset} \sigma^{4-q}\mathrm{d}G \leq \left(\int\limits_{D\cap G\neq\emptyset} \sigma^{4}\mathrm{d}G\right)^{1-\frac{q}{4}} \left(\int\limits_{D\cap G\neq\emptyset} 1\mathrm{d}G\right)^{\frac{q}{4}}. \quad (14)$$

Application of (6) and (8) yields the result.

One arrives at both lower and upper bounds of the MRP for the special case $\rho=0$

$$\frac{2\kappa}{(3-q)(4-q)}2^{7-2q}\pi V^{2-q}A^{q-3} \leq I_q \leq \frac{2\kappa}{(3-q)(4-q)}6^{1-\frac{q}{4}}\left(\frac{\pi}{2}\right)^{\frac{q}{4}} \times V^{-\frac{q}{2}}A^{\frac{q}{4}}\ (q<3). \quad (15)$$

References

[1] H. Hashemi, "The indoor radio propagation channel," *Proc. IEEE*, vol. 81, no. 7, pp. 943–968, July 1993.

[2] J. Lansford, R. Nevo, and B. Monello. (2001, May) Wi-Fi and Bluetooth: enabling coexistance. *Compliance Eng.* [Online]vol. www.ce-mag.com

[3] T. S. Rappaport, S. Y. Seidel, and K. Takamizawa, "Statistical channel impulse response models for factory and open plan building radio communication system design," *IEEE Trans. Commun.*, vol. 39, pp. 794–807, May 1991.

[4] S. Y. Seidel and T. S.Th. S. Rappaport, "Site-specific propagation prediction for wireless in-building personal communication system design," *IEEE Trans. Veh. Technol.*, vol. 43, pp. 879–891, Nov. 1994.

[5] COST 207 Management Committee, COST 207: Digital land mobile radio communications (Final Report), Commission of the European Communities, 1989.

[6] R. Heddergott, U. P. Bernhard, and B. H. Fleury, "Stochastic radio channel model for advanced indoor mobile communication systems," in *Proc. 8th IEEE Int. Symp. Personal, Indoor and Mobile Radio Communications (PIMRC,'97)*, vol. 1, Helsinki, Finland, Sept. 1997, pp. 140–144.

[7] COST 259 Management Committee, COST 259: Wireless flexible personalised communications (Final Report), Commission of the European Communities, 2001.

[8] T. Zwick, C. Fischer, D. Didascalou, and W. Wiesbeck, "A stochastic spatial channel model based on wave-propagation modeling," *IEEE J. Select. Areas Commun.*, vol. 18, pp. 6–15, Jan. 2000.

[9] M. Hassan-Ali and K. Pahlavan, "A new statistical model for site-specific indoor radio propagation prediction based on geometrical optics and geometric probability," *IEEE Trans. Wireless Commun.*, vol. 1, pp. 112–124, Jan. 2002.

[10] L. Santalo, *Integral Geometry and Geometric Probability*. London, U.K.: Addison-Wesley, 1976.

[11] H. Solomon, *Geometrical Probability*. Philadelphia, PA: SIAM, 1978.

[12] M. G. Kendall and P. A. P. Moran, *Geometrical Probability*. London, U.K.: Charles Griffin, 1963.

[13] A. Papoulis, *Probability, Random Variables and Stochastic Processes*. New York: McGraw-Hill, 1965.

[14] J. Hansen, "A novel stochastic millimeter wave indoor radio channel model," *IEEE J. Select. Areas Commun.*, vol. 20, pp. 1240–1246, Aug. 2002.
[15] T. S. Rappaport, *Wireless Communications*. New York: IEEE Press, 1996.
[16] W. C. Y. Lee, *Mobile Communication Design Fundamentals*. New York: Wiley, 1993.
[17] J. D. Gibson, *Mobile Communications*. New York: IEEE Press, 1996.
[18] N. W. Ashcroft and N. D. Mermin, *Solid State Physics*. Philadelphia, PA: Saunders College, 1976.
[19] L. D. Landau and E. M. Lifschitz, *Lehrbuch der Theoretischen Physik, Band 5*. Berlin, Germany: Akademie Verlag, 1966.
[20] W. Blaschke, "Eine isoperimetrische Eigenschaft des Kreises," *Mathematische Zeitschrift*, vol. 1, pp. 52–57, 1918.
[21] T. Carleman, "Über eine isoperimetrische Aufgabe und ihre physikalischen Anwendungen," *Mathematische Zeitschrift*, vol. 3, pp. 1–7, 1919.
[22] A. M. Mathai, *Introduction to Geometrical Probability*. Amsterdam, The Netherlands: Gordon and Breach, 1999.
[23] M. W. Crofton, "Probability," in *Encyclopaedia Britannica*, 9th ed., 1885, vol. 19, pp. 768–788.
[24] R. V. Ambartzumjan, J. Mecke, and D. Stoyan, *Geometrische Wahrscheinlichkeiten und Stochastische Geometrie*. Berlin, Germany: Akademie Verlag, 1993.
[25] R. Schneider and J. Wieacker, "Integral geometry," in *Handbook of Convex Geometry*. Amsterdam, The Netherlands: Elsevier Science, 1993.
[26] H. Alt, *Lineare Funktionalanalysis*, 3rd ed. Berlin: Springer, 1999.
[27] E. Zollinger, "Eigenschaften von Funkübertragungsstrecken in Gebäuden," Ph.D. dissertation, Swiss Federal Institute of Technology, Zurich, 1993.
[28] A. von Hippel, *Dielectric Materials and Applications*. New York: Wiley, 1954.
[29] N. Geng and W. Wiesbeck, *Planungsmethoden für die Mobilkommunikation*. Berlin, Germany: Springer Verlag, 1998.

Jan Hansen (S'00) received the B.Sc. degree in physics/mathematics from Trent University, Peterborough, Canada, in 1995 and the diploma degree in physics from Freiburg University, Germany, in 1998. He is currently pursuing the Ph.D. degree.

In 1998, he joined the Communication Technology Laboratory, ETH Zurich, Switzerland.

Peter E. Leuthold (M'68) received the diploma and Ph.D. degrees in electrical engineering from ETH Zurich, Switzerland, in 1962 and 1967, respectively.

From 1964 to 1967, he was an Associate Member of Technical Staff, Philips Research Laboratories, Eindhoven, the Netherlands. In 1968, he joined the Research Staff of the High Frequency Electronics Laboratory, ETH Zurich, where he worked on multidimensional digital filter structures and their application in data modems. From 1974 to 1977, he was a full-time Lecturer at Intercantonal Engineering College, Rapperswil. Since fall 1977, he has been a Professor at ETH Zurich. He was Head of the Communication Technology Laboratory from 1979 to 2002. His research interests include mobile radio communications and fiber-optical networks.

Dr. Leuthold has organized several international conferences on telecommunications and electromagnetic compatibility and was General Chairman of ICC'93 in Geneva.